

Automatic Classification of Images with Appendiceal Orifice in Colonoscopy Videos

Yu Cao, Danyu Liu, Wallapak Tavanapong, Johnny Wong, JungHwan Oh, and Piet C. de Groen

Abstract—Colonoscopy is an endoscopic technique that allows a physician to inspect the inside of the human colon. In current practice, videos captured from colonoscopic procedures are not routinely stored for either manual or automated post-procedure analysis. In this paper, we introduce new algorithms for automated detection of the presence of the shape of the opening of the appendix in a colonoscopy video frame. The appearance of the appendix in colonoscopy videos indicates traversal of the colon, which is an important measurement for evaluating the quality of colonoscopic procedures. The proposed techniques are valuable for (1) establishment of an effective content-based retrieval system to facilitate endoscopic research and education; and (2) assessment and improvement of the procedural skills of endoscopists, both in training and practice.

I. INTRODUCTION

COLORECTAL cancer is the second leading cause of cancer-related deaths behind lung cancer in the United States [1]. As the name implies, colorectal cancers are malignant tumors that develop in the colon and rectum. The survival rate is higher if the cancer is found and treated early before metastasis to lymph nodes or other organs occurs.

Colonoscopy is currently the preferred screening modality for prevention of colorectal cancer. During a colonoscopic procedure, a flexible endoscope (with a tiny video camera at the tip) is gradually advanced under direct vision via the anus and rectum into the most proximal part of the colon (signified by the appearance of the appendiceal orifice or the terminal ileum). Next, the endoscope is gradually withdrawn. The video camera generates a sequence of images (frames) of the internal mucosa of the colon. These images are displayed on a monitor for real-time manual analysis by the endoscopist. Biopsy and therapeutic operations such as polyp removal can be performed during the procedure.

Colonoscopy has resulted in a decline in the number of colorectal cancer related deaths. Nevertheless, recent data from clinical trials suggest that there is a significant miss-rate for detection of both large polyps and cancers [2]. The miss-rate may be related to the experience of the endoscopist

and the location of the lesion in the colon, but no large prospective studies related to this have been done thus far.

We have recently developed: (i) a system to capture all images from a colonoscopic procedure into a colonoscopy video file in MPEG-2 format; (ii) new audio and/or visual analysis techniques to identify biopsy and therapeutic operations from colonoscopy videos [3]; and (iii) image/video analysis techniques that output objective measures of quality of colonoscopic procedures such as portion of clear images seen during the withdrawal of the endoscope [4]. The presence of a sufficient number of images showing a closely inspected appendiceal orifice (see Fig. 1(c-d)) is one of the important objective indicators that the most proximal end of the colon has been reached during the procedure. Other indicators include presence of small bowel mucosa and ileocecal valve. Reaching the end of the colon is one of the prerequisites for complete inspection; an incomplete inspection may be due to poor colon preparation, inability to reach the proximal colon end or inability of the endoscopist to visualize all mucosa.

In this paper, we call an image with a closely inspected appendiceal orifice an “appendix image”. We classify images in a colonoscopy video into two categories: *appendix image class* and *non-appendix image class*. To the best of our knowledge the question of whether or not an image contains the shape of the opening of the appendix has not been investigated in the literature. The answer to this question may have a significant impact for patient care. That is, if few or no appendix images are found in a colonoscopy video, the video may require a manual second opinion to determine whether the complete colon indeed was visualized. If this is not the case, the patient may have to undergo a second procedure. The appendix frame classification problem is very challenging due to different view angles and locations of the appendiceal orifice, partial or near complete removal after appendectomy, presence of stools occluding the appendiceal orifice, presence of strong light reflected spots, presence of out-of-focus images, and biopsy and therapeutic instruments.

Our experience using commonly used low-level features (color, texture, and generic shape descriptors) or salient features detected using a recent salient feature detection technique for generic objects [5] indicate that these techniques do not give good results for this problem. In this paper, we propose several new intermediate level features suitable for the appendix image classification problem.

The rest of the paper is organized as follows. In Section II, we briefly review recent related work. We present our proposed solution in Section III and report the effectiveness

This work was supported in part by the U.S. National Science Foundation under Grant IIS-0513777, IIS-0513809, and IIS 0513582 and the Mayo Clinic.

Y. Cao, D. Liu, W. Tavanapong, and J. Wong are with the Department of Computer Science, Iowa State University, Ames, IA 50011, USA (e-mail: impact.isu@cs.iastate.edu).

J. Oh is with the Department of Computer Science and Electrical Engineering, University of Texas at Arlington, TX 76019-0015, USA (e-mail: oh@cse.uta.edu).

P. C. de Groen is with Mayo Clinic College of Medicine, Mayo Clinic, Rochester, MN 55905, USA.

of the proposed technique in Section IV. Finally, we provide conclusions and a description of future work in Section V.

II. RELATED WORK

Recent years have seen research on techniques for guiding a colonoscope during a colonoscopic procedure [6], development of colonoscope hardware [7], analyses of microscopic images from biopsies of colon tissues [8], analyses of images from colonoscopic procedures for tumor detection [9, 10], and virtual colonoscopy [11]. Most research efforts have focused on detecting an abnormality or specific object in a single frame; few have addressed image recognition in continuous endoscopic frames as present in colonoscopy videos.

Several techniques for object class recognition have also been proposed in recent years [12, 13]. These techniques recognize object categories. Each object category is represented by local features, global features, or a hybrid of them. None of the existing object class recognition techniques have been proposed or applied to the recognition of the appendix image class.

III. PROPOSED APPROACH

Our image classification technique consists of two steps. First, we obtain from each image intermediate features that we introduce in this paper. Second, we use K-mean classifier to finally group the images into two groups: *appendix image class* and *non-appendix image class*. We derive the new intermediate features based on the following two observations: 1) *When the appendix is closely inspected, a distant colon lumen is not visible (“no colon lumen”)*; 2) *The clearly seen appendix orifice has several curvilinear structures that are part of ellipses. These structures usually are located in the center of the image when the appendix is the focal point of inspection.*

The new features are as follows (1) Likelihood of no colon lumen; (2) Ratio of edge pixels that are part of curvilinear structures; (3) Coverage of the ellipse inside the image; (4) Ratio of edge pixels that are part of ideal ellipses. We describe the derivation of these features in more detail below.

1) *Feature representing the likelihood of no colon lumen:* Based on the first observation, this feature represents the possibility of the presence of distant lumen in the image. We first segment the image using JSEG [14]. The segmented image contains multiple regions, as shown in Fig 1(b) and Fig 1(d). The likelihood of no distant colon lumen is computed as follows.

$$P_{NoLumen} = \frac{I_{Darkest\ Region}}{I_{Max}}, \text{ where}$$

$P_{NoLumen}$ is the likelihood of no distant colon lumen, $I_{Darkest\ Region}$ is the average intensity of the darkest region, and I_{Max} is the maximal intensity of the image. The darkest regions are pointed out by the arrows in Fig. 1(b) and Fig. 1(d). Generally, the value of $P_{NoLumen}$ for an appendix image is larger than that of the image with distant colon lumen since

the average intensity value of the darkest region of appendix image is larger than the value of images with “dark” distant lumen. Fig. 1 shows the visual difference between the image with distant lumen and the appendix image. Note that the small size regions are removed by filtering out all the regions

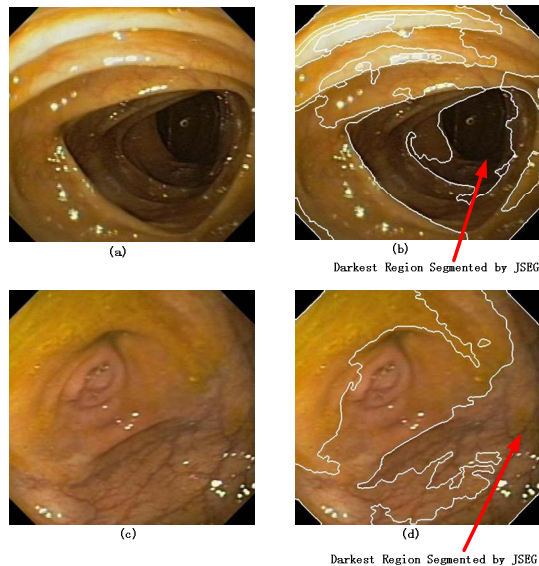


Fig. 1. Image examples before and after segmentation: (a) Original lumen image, (b) Lumen image after segmentation, (c) Original appendix image, (d) Appendix image after segmentation. The average intensity of the darkest region for the lumen image is much smaller than the one for the appendix image, which is consistent with our observation (1)

whose size is less than a pre-defined size threshold.

2) *Feature representing the ratio of edge pixels belonging to curvilinear structure:* Based on the second observation, an appendix image has several curvilinear structures. We claim that the possibility that the image contains the appendiceal orifice is high if the many edge pixels belong to curvilinear structures corresponding to the appendiceal orifice. To get the edge image that includes the curvilinear structures, we employ the same Hessian matrix-based technique used previously [3]. In Fig. 2, the binary image (Fig. 2(b)) contains ellipse-shape curves that are part of the appendiceal orifice. But it also includes other curves, as shown in the bottom right part of Fig 2(b). We select the true appendix curve by checking the curvature change along the skeleton of each curve. The skeleton of the curve that is not a real appendiceal orifice has either a small curvature change (curve with linear shape, illustrated as the left curve of the two curves in the right bottom of Fig 2(b)) or a very large curvature change (curve with round shape, illustrated as the right curve of the two curves in the right bottom of Fig 2(b)).

After the above preprocessing step, we compute the value of edge pixels in the curvilinear structures corresponding to the appendiceal orifice over the total number of edge pixels in the binary image.

$$R_{Curve} = \frac{EdgeNum_{Curve}}{EdgeNum_{Img}}, \text{ where}$$

R_{Curve} indicates the ratio of edge pixels of the appendix curvilinear structures; $EdgeNum_{Curve}$ is the number of edge pixels that belong to the curvilinear structures of the appendix orifice. $EdgeNum_{img}$ is the number of edge pixels in the entire image. In Fig. 2(b), many edge pixels in the binary image (generated from the appendix image) are curves corresponding to the appendiceal orifice. But most edge pixels in Fig. 2(d) are curves that are not part of the appendiceal orifice. A large value of R_{Curve} indicates a high probability that the appendiceal orifice is present in the image.

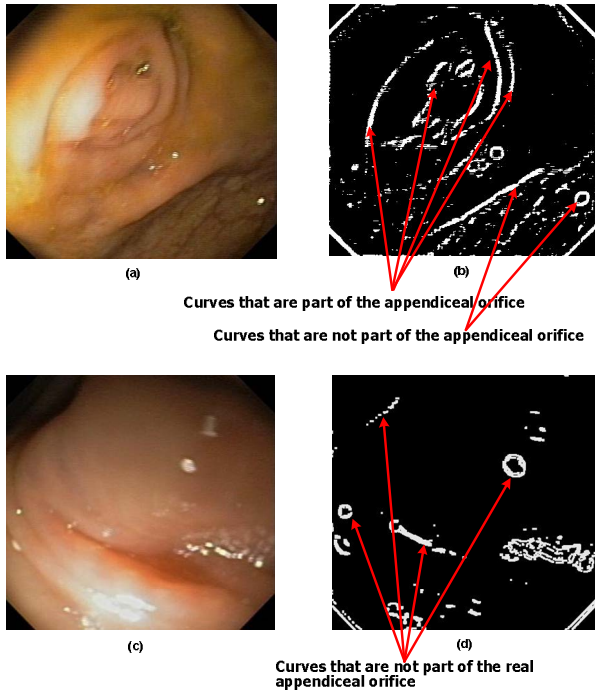


Fig. 2 Image examples for image enhancement based on Hessian Matrix: (a) Original appendix image, (b) Edge image after enhancement, (c) Original image without a clearly seen appendiceal orifice, (d) Edge image after enhancement

3) *Features representing partial ellipses in an image:* Recall our second observation that a closely inspected appendiceal orifice has several curvilinear structures that are part of ellipses. To derive the two features that reflect this observation, we only consider curves that are potential candidates for the true appendiceal orifice from the computation of the previous feature (e.g., curve ACu in Fig. 3). We want to find an ideal ellipse with certain part fitting well with the candidate curve. For example, part of the ideal ellipse A fits well with curve ACu as shown in Fig. 3. We introduce a new modification to the randomized Hough Transform [15] abbreviated to MHT. MHT works as follows. Given an edge image with a curve, say ACu , we expand the image and get the skeleton Ske_{ACu} of the curve. Then, we perform a boundary tracing algorithm on Ske_{ACu} to get a boundary represented by a sequence of points $\{P_1, \dots, P_i, P_{i+1}, \dots, P_n\}$ where P_i and P_{i+1} are neighboring edge pixels. Next, we divide the sequence of points into three segments with equal length, illustrated in Fig. 3. We generate an ideal

ellipse as follows. We randomly pick one edge pixel from each segment and compute an ideal ellipse whose boundary passes the three chosen edge pixels in a polar coordinate. The ideal ellipse is represented by an *ellipse tuple* (x, y coordinates of the ellipse centroid, the length of the major axis, the length of the minor axis, and the orientation of the major axis). If at least 90% of the edge pixels of the curve are on the boundary of the ideal ellipse, we consider this ellipse as a valid ideal ellipse for the curve and stop the MHT for this curve. Otherwise, we continue to select three random pixels from the three segments and repeat the above procedure. If we can not find any valid ellipse after N iterations where N is a predefined threshold, we skip this curve.

As shown in Fig. 4, the ideal ellipse (*Ellipse A and Ellipse B*) may or may not be enclosed entirely in the original image. The more curvilinear structures we find in the boundary of the ideal ellipse, the more likely the appendiceal orifice is present in the image.

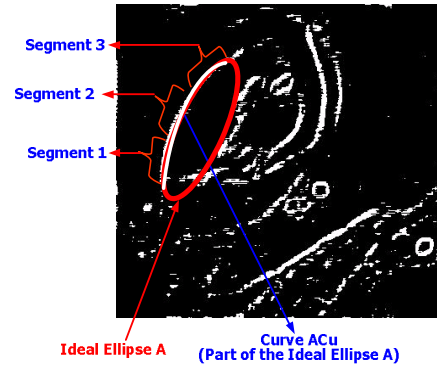


Fig. 3. Derivation of the ideal ellipse A from curve ACu , which is part of the ideal ellipse A and resides in the boundary of ellipse A

After this step, we get a number of ideal ellipses. We eliminate any detected ellipse with less than 50% of its area

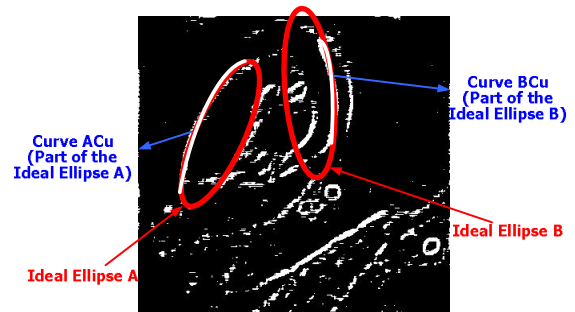


Fig. 4. Relationship between the appendix curve and ideal ellipse

inside the original image. We compute “Ellipse Coverage ($COV_{Ellipse}$)” to reflect the amount of the ellipse area inside the original image. Let k be the number of valid ellipses. Let $PixelNumInsideOriImg_i$ be the number of pixels that are both inside the ellipse i and inside the original image and $PixelNumInsideEllipse_i$ is the number of pixels inside the ellipse i , where $i \in \{1..k\}$. Combining this we have the following equation for the ellipse coverage.

$$COV_{Ellipse} = \frac{\sum_{i=1}^k PixelNumInsideOriIm g_i}{\sum_{i=1}^k PixelNumInsideEllipse_i}$$

If this value is high, we can find many ideal ellipses with most of their area inside the original image. Hence, the possibility of the presence of an appendix is high.

We introduce another feature called ‘‘Ellipse Edge Coverage ($COV_{EllipseEdge}$)’’ computed as follows.

$$COV_{EllipseEdge} = \frac{\sum_{i=1}^k EdgeNumOnEllipseBoundary_i}{\sum_{i=1}^k TotalPixelNumOnEllipseBoundary_i}, \text{ where}$$

$EdgeNumOnEllipseBoundary_i$ is the number of pixels on the appendix curve that is on the boundary of ellipse i , and $TotalPixelNumOnEllipseBoundary_i$ is the total number of pixels on the boundary of ellipse i , where $i \in \{1..k\}$. If this value is high, many ideal ellipses are present with the majority of their boundaries covered by the curvilinear structures of the appendiceal orifice. Thus, an appendix image has a high value of $COV_{EllipseEdge}$.

For each video, we extract the four intermediate features for each image and apply a K-means classifier. Euclidean distance function and equal weight for each feature are used for K-means classifier. Since our goal is to classify the colon image into two types, we set K to two. Any image in this video will be classified as either an appendix image or a non-appendix image.

IV. EXPERIMENTAL RESULTS

We implemented the classification algorithm in MATLAB. A test image set was created that consisted of about 800 images from 5 colonoscopy videos: the images were manually classified as either appendix or non-appendix images (see Table I). We report the percentage of images that are correctly classified for each class using our technique in Table II. As can be seen, our technique has an average accuracy of 90% for appendix images and 90% for non-appendix images.

V. CONCLUSION AND FUTURE WORK

Our initial results suggest that the four features we used are promising, but also that there is ample room for improvement. Several appendix images were missed because the angle of view distorted the elliptical shape of the appendiceal orifice. Others were missed because the appendiceal orifice was located at the edge of the image. Our technique falsely classified several non-appendix images as appendix images due to a very large light reflecting area, or due to anatomic mucosal appearances with characteristics similar to those of the appendiceal orifice. In addition, our test set does not contain images with much stool in them. To handle a large light reflected areas and the presence of stool, we will need to pre-process the images before applying the classification algorithm. We plan to improve our technique by using additional features such as absence of further forward movement and a more advanced classifier.

TABLE I
CHARACTERISTIC OF THE IMAGE SET

Video ID	Number of Appendix Images	Number of Non-appendix images
00903	34	116
01003	27	132
04703	9	109
04706	24	209
04806	8	99

TABLE II
EFFECTIVENESS OF IMAGE CLASSIFICATION

Video ID	Accuracy for Appendix Images	Accuracy for Non-appendix images
00903	0.85	0.91
01003	0.92	0.93
04703	1.00	0.86
04706	0.88	0.89
04806	0.88	0.87
Average	0.90	0.90

REFERENCES

- [1] A. C. Society, ‘‘Colorectal Cancer Facts & Figures,’’ American Cancer Society, 2005.
- [2] D. L. (Editorial), ‘‘Quality and Colonoscopy: a New Imperative,’’ *Gastrointestinal Endoscopy*, vol. 61, 2005.
- [3] Y. Cao, D. Liu, W. Tavanapong, J.-H. Oh, J. Wong, and P.C. de Groen, ‘‘Computer-aided Detection of Biopsy and Therapeutic Operations in Colonoscopy Videos,’’ *Submitted to IEEE Trans. on Biomedical Engineering*.
- [4] S. Hwang, J. Oh, J. Lee, Y. Cao, W. Tavanapong, D. Liu, J. Wong, and P.C. de Groen, ‘‘Automatic Measurement of Quality Metrics for Colonoscopy Videos,’’ *Proc. of ACM Multimedia, Singapore, 2005*, pp. 912-921.
- [5] D. Lowe, ‘‘Distinctive Image Features from Scale-Invariant Keypoints,’’ *Int'l Journal of Computer Vision*, vol. 60, 2004.
- [6] S. J. Phee and W. S. Ng, ‘‘Automatic of colonoscopy: Visual control aspects,’’ in *IEEE Eng. in Medicine and Biology Magazine*, vol. 17, 1998.
- [7] N. O. Khessal and T. M. Hwa, ‘‘The Development of an Automatic Robotic Colonoscope,’’ *Proc. of TENCON, 2000*, vol. 2, pp. 71-76.
- [8] N. Esgiar, R. N. G. Naguib, B. S. Sharif, M. K. Bennett, and A. Murray, ‘‘Microscopic Image Analysis for Quantitative Measurement and Feature Identification of Normal and Cancerous Colonic Mucosa,’’ *IEEE Trans Info Tech. Biomed*, vol. 2, pp. 197-203, 1998.
- [9] S. A. Karkanis, D. K. Iakovidis, D. E. Maroulis, D. A. Karras, and M. Tzivras, ‘‘Computer-Aided Tumor Detection in Endoscopic Video Using Color Wavelet Features,’’ *IEEE Trans. on Information Technology in Biomedicine*, vol. 7, 2003.
- [10] G. D. Magoulas, V. P. Plagianakos, D. K. Tasoulis, and M. N. Vrahatis, ‘‘Tumor Detection in Colonoscopy using the Unsupervised K-windows Clustering Algorithm and Neural Networks,’’ *Proc. of European Symposium on Biomedical Engineering, 2004*.
- [11] A. Kaufman, S. Lakare, I. Bitter, and K. Kreeger, ‘‘Virtual Colonoscopy,’’ in *Communications of the ACM*, vol. 48, 2005, pp. 37-41.
- [12] R. Fergus, P. Perona, and A. Zisserman, ‘‘Object class recognition by unsupervised scale-invariant learning,’’ *Proc. of Computer Vision and Pattern Recognition, 2003*.
- [13] W. Zhang, B. Yu, G. Zelinsky, and D. Samaras, ‘‘Object class recognition using multiple layer boosting with multiple features,’’ *IEEE Proc. of CVPR, 2005*, pp. 323-330.
- [14] Y. Deng and B. S. Manjunath, ‘‘Unsupervised segmentation of color-texture regions in images and video,’’ *IEEE Trans. on Pattern Analysis and Machine Intelligence*, 2001.
- [15] P. K. L. Xu and E. Oja, ‘‘A new curve detection method: Randomized hough transform,’’ *Pattern Recognition Letters*, vol. 11, pp. 331-338, 1990.